International Journal of Nanomedicine

Dovepress
open access to scientific and medical research

Open Access Full Text Article

ORIGINAL RESEARCH

Cytotoxicity of gold nanoclusters in human liver cancer cells

This article was published in the following Dove Press journal:
International Journal of Nanomedicine
25 November 2014
Number of times this article has been viewed

Yanjie Yang[1,2]
Jing Nan[3]
Jianwen Hou[3]
Bianfei Yu[1]
Tong Zhao[1]
Shuang Xu[1]
Shuangyu Lv[2]
Haixia Zhang[1]

[1]Key Laboratory of Nonferrous Metal Chemistry and Resources Utilization of Gansu Province, Lanzhou University, Lanzhou, [2]School of Medicine, Henan University, Kaifeng, [3]School of Life Sciences, Lanzhou University, Lanzhou, People's Republic of China

Abstract: In this study, we synthesized water-soluble fluorescent gold nanoclusters (Au NCs) stabilized with dihydrolipoic acid (DHLA). The cytotoxicity of these Au NCs was then assessed in the normal human hepatic cell line (L02) and the human hepatoma cell line (HepG2) at different exposure times. Cell viability was normal in both cell lines at 24 hours and 48 hours; however, the growth of HepG2 cells was significantly inhibited at 72 hours. The change in lactate dehydrogenase level was strongly correlated with cell viability after 72 hours incubation with DHLA–capped Au NCs, and the increase in cellular reactive oxygen species may be related to the decrease in cell viability. Growth inhibition of HepG2 cells was possibly due to difficultly passing the checkpoint between G1 phase and S phase. The anticancer activity of DHLA–capped Au NCs should be considered when used in biomedical imaging and drug delivery.

Keywords: gold nanocluster, cytotoxicity, cell viability, reactive oxygen species, cell cycle

Introduction

Noble metal nanoclusters (NCs) such as Au and Ag, typically consist of several to tens of atoms and have an ultra small size (≤2 nm) comparable to the Fermi wavelength of free electrons.[1,2] Gold nanoclusters (Au NCs) have bright fluorescence ranging from ultraviolet to the near-infrared region depending on the cluster size and composition.[1,3] Due to their ultra small size, excellent luminescence properties, and stable structures, Au NCs have attracted significant attention in the past decade.[2–5] Chen et al[6] determined the enzyme activity by assessing the change in emission intensity of fluorescent Au NCs, Qiao et al[7] reported that ovalbumin-protected Au NCs with folic acid can be used for HeLa cells imaging, and Yue et al[8] synthesized bovine serum albumin–capped Au NCs as a fluorescence probe to determine nitrite (NO_2^-) sensitively and selectively.

Inorganic nanoparticles are difficult to biodegrade and induce long-term toxicity, which hinders their application in clinical practice.[9] Particles smaller than 5.5 nm can be rapidly and efficiently removed by the kidneys,[9,10] which allows them to be used safely in the clinic. Recently, Zhang et al[10] reported that the renal clearance rate of glutathione-protected Au NCs (2.1 nm) was maximum at 2 hours after injection, and only 6% of Au could be detected in mice at 28 days.

With the development of nanoparticle application, it is necessary to assess their potential toxicity to avoid adverse effects in humans and the environment.[11] Liu et al[12] found that bare $Au_{55}(Ph_2PC_6H_4SO_3H)_{12}Cl_6$ combined irreversibly into the major grooves of B-DNA (depth: 0.9 nm; length: 1.43 nm) due to their distinct size of 1.4 nm. Subsequently, Tsoli et al[13] reported that the IC_{50} (half maximal inhibitory concentration) of $Au_{55}(Ph_2PC_6H_4SO_3H)_{12}Cl_6$ was approximately 180 times lower than the anticancer drug cisplatin in BLM melanoma cells and more than 200 times lower in the MV3 cell line.

Correspondence: Haixia Zhang
Key Laboratory of Nonferrous Metal Chemistry and Resources Utilization of Gansu Province, Lanzhou University, 222 Tianshui South Road, Lanzhou 730000, People's Republic of China
Tel +86 931 891 2510
Fax +86 931 891 2582
Email zhanghx@lzu.edu.cn

Besides, the toxicity of Au_{55} in osteosarcoma cell lines (SK-ES-1 and U-2OS) was higher than healthy cell line (MC3T3-E1). Oh et al[14] have also found that Au NCs elicit cytotoxicity in the cellular viability test using COS-1 cell line.

Liver, as reticuloendothelial system, is the primary exposure site to foreign compounds.[15] Moreover, results from in vivo assay showed that Au NCs were mainly accumulated in the liver.[10,16] Shang et al[3] developed a one-pot synthetic strategy to synthesize water-soluble dihydrolipoic acid (DHLA)–capped Au NCs, which are promising imaging agents for biomedical and cellular imaging. In the present study, we selected the normal human hepatic cell line (L02) and hepatoma cell line (HepG2) to investigate the cytotoxicity of DHLA–Au NCs.

Materials and methods

Chemicals

Lipoic acid, sodium borohydride, and $HAuCl_4$ were supplied by Sinopharm Chemical Reagent Co Ltd (Shanghai, People's Republic of China). Fetal bovine serum was purchased from Sijiqing, (Hangzhou, People's Republic of China). RPMI 1640 medium was purchased from HyClone Laboratories (Logan, UT, USA). Trypsin and dimethyl sulfoxide (DMSO) were obtained from Sigma-Aldrich (St Louis, MO, USA). 3-(4,5-Dimethylthiazol-2-yl)-2,5-diphenyltetrazolium bromide (MTT) and RNase A were provided by Sangon Biotech (Shanghai, People's Republic of China). Deionized water was prepared from EMD Millipore (Billerica, MA, USA). Other reagents used were of analytical grade.

Preparation and characterization of DHLA–capped Au NCs

DHLA–capped Au NCs were synthesized following a previously reported method.[3] Briefly, 100 μL of NaOH (2 M) and 39 mL of deionized water were mixed in a flask and then 13 mg of lipoic acid was added and stirred for 15 minutes at room temperature (approximately 25°C). To the mixture, 400 μL of $HAuCl_4$ (2% by mass) was added and stirred for another 5 minutes until colorless. Finally, 800 μL of aqueous solution of sodium borohydride (50 mM) was added slowly with stirring. After 12 hours of stirring, the resulting DHLA–capped Au NCs were purified by dialysis (molecular weight cut off was 3 kDa) for 72 hours and dried in vacuum.

Transmission electron microscopy images were measured with JEM-2100 (JEOL, Tokyo, Japan). Absorption spectra were measured with a Puxi TU-1810 visible spectrophotometer (Beijing, People's Republic of China). Fluorescence spectra were determined by RF-5301PC fluorescence spectrometer (Shimadzu, Kyoko, Japan). The size distribution was carried on dynamic light scattering using a BI-200SM (Brookhaven Instruments Corporation, Holtsville, NY, USA). Zeta potentials were recorded on a Zetasizer Nano 3600 (Malvern Instruments Ltd, Malvern, UK).

Cell culture

The normal human hepatic cell line (L02) and the human HepG2 were provided by the Cell Bank of Shanghai Institute of Biochemistry and Cell Biology, Chinese Academy of Sciences (Shanghai, People's Republic of China). Both were cultured in RPMI 1640 medium containing 10% fetal bovine serum and 1% penicillin–streptomycin. The cell lines were maintained at 37°C in a humidity- and CO_2-controllable incubator (Thermo Forma, Marietta, OH, USA) with 5% CO_2, and all the experiments were performed in a clean atmosphere.

Cell viability assay

Cell viability was determined by the colorimetric MTT assay, in which water-soluble MTT was reduced to undissolved blue formazan dye within viable cells. Both L02 and HepG2 cells were seeded into 96-well plates (5.0×10^3 cells per well) and incubated at 37°C for 24 hours, and DHLA–capped Au NCs in RPMI 1640 medium were added at final concentrations of 12.5 μM, 25 μM, 50 μM, 75 μM, 100 μM, and 125 μM. At the end of the fixed incubation period (24 hours, 48 hours, and 72 hours), the culture medium was discarded and 20 μL of MTT reagent (diluted in culture medium, 0.5 mg/mL) was added. After 4 hours incubation at 37°C, MTT/medium was removed, and the plates were carefully washed with phosphate-buffered saline (PBS). To dissolve the formazan crystals, 150 μL of DMSO was added and incubated for 30 minutes, and the absorbance at 490 nm was recorded using a microplate reader. All experiments were performed in triplicate.

Lactate dehydrogenase assay

Lactate dehydrogenase (LDH) is a stable cytoplasmic enzyme and is released into cell culture medium when the plasma membrane is damaged due to either apoptosis or necrosis. Accordingly, LDH activity can be regarded as an indicator of cell membrane integrity and used to assess the cytotoxicity caused by chemical compounds or other toxic environmental factors. HepG2 cells (5.0×10^3 cells per well) were incubated with different concentrations of DHLA–capped Au NCs (12.5 μM, 25 μM, 50 μM, 75 μM, 100 μM, and 125 μM) for 72 hours and then centrifuged (800 rpm, 5 minutes,

Eppendorf 5810R centrifuge) and 120 μL of culture supernatant was collected. LDH levels were determined according to commercial kit protocols (Beyotime, Shanghai, People's Republic of China). Absorption was measured using a microplate reader at 490 nm.

Reactive oxygen species

Reactive oxygen species (ROS) were determined using 2′,7′-dichlorodihydrofluorescein diacetate (DCFH-DA) according to the kit protocol. DCFH-DA has no fluorescence and can enter the plasma membrane passively, where it is then converted to DCFH by intracellular esterase. DCFH cannot cross the membrane and is converted to the highly fluorescent derivative dichlorofluorescein after being oxidized by ROS. A total of 5.0×10^3 HepG2 cells per well were cultured with or without DHLA–capped Au NCs for 72 hours. After three washes, 10 μM of DCFH-DA working solution was added, and the cells were incubated for 20 minutes at 37°C. The plates were then washed three times to remove DCFH-DA. Fluorescence intensity was detected using a microplate counter at an excitation wavelength of 488 nm and an emission wavelength of 525 nm.

Cell cycle assay

Determination of the cell cycle was carried out by staining the DNA with propidium iodide, followed by the assessment of fluorescence by flow cytometry. HepG2 cells were seeded in 6-well plates (1.0×10^5 cells per well) and treated with the culture medium (control), 25 μM and 100 μM DHLA–capped Au NCs for 72 hours. The cells were washed three times with PBS, harvested using 0.25% trypsin, fixed in prechilled 70% ethanol overnight at 4°C, incubated for 30 minutes in 20 mg/L RNase A, and then stained with propidium iodide at a final concentration of 20 mg/L for 30 minutes. The cell cycle was analyzed by flow cytometry and calculated using ModFit LT version 3.1 software.

Statistical analysis

All the data were presented as mean ± standard error of the mean. Multiple group comparisons of the means were evaluated by one-way analysis of variance using SPSS 16.0, and $P<0.05$ was considered statistically significant.

Results

Characterization of DHLA–capped Au NCs

The DHLA–capped Au NCs were synthesized using the one-pot synthesis method as reported in the literature[3] and their characteristics are shown in Figure 1. The UV–vis absorption bands were located at 505 nm and 560 nm as in the previous report,[3] and the 520-nm absorbance peak of surface plasmon resonance was not observed (Figure 1A). The photoluminescence spectra of DHLA–capped Au NCs are described in Figure 1B, in which the maximum emission peak was centered at 660 nm following excitation at 550 nm. Dynamic light scattering was also used to determine the size of DHLA–capped Au NCs (Figure 1C), and the average hydrodynamic diameter was 3.32±0.62 nm. The core structures of DHLA–capped Au NCs was shown in the transmission electron microscopy micrograph, and the average core size was 1.5±0.1 nm (Figure 1D). Zeta potential is usually used to estimate surface charge and predict the stability of the suspension. Our DHLA–capped Au NCs in deionized water showed a negative charge of −26.9 mV.

Cell viability in the presence of DHLA–capped Au NCs

DHLA–capped Au NCs had no effect on the viability of L02 cells and HepG2 cells even at the high concentration of 100 μM after 24 hours and 48 hours of exposure (Figure 2A and B). At 72 hours, the viability of DHLA–capped Au NC–treated L02 cells was 98.75%±3.16% versus control ($P>0.05$), while the viability of HepG2 cells decreased significantly at the concentration of 50 μM (78.65%±0.44% versus control, $P<0.01$), and only 44.42%±0.80% ($P<0.001$) of control cells survived at the maximal dose of 125 μM (Figure 2C).

LDH leakage caused by DHLA–capped Au NCs

As shown in Figure 3A, LDH leakage in HepG2 cells increased in a concentration-dependent manner after 72 hours of exposure. A statistically significant difference in LDH concentration was observed at 50 μM (155.86%±2.63% versus control, $P<0.01$), which was in accordance with the cell viability results. LDH leakage was 213.37%±5.91% ($P<0.001$) of the control at the highest concentration of DHLA–capped Au NCs (125 μM). There was a strong correlation between decreased cell viability and increased LDH activity ($R^2=0.961$) after 72 hours incubation with DHLA–capped Au NCs (Figure 3B).

Oxidative stress induced by DHLA–capped Au NCs

Figure 4 shows that the fluorescence intensity of dichlorofluorescein in HepG2 cells was elevated with increasing concentrations of DHLA–capped Au NCs up to 50 μM

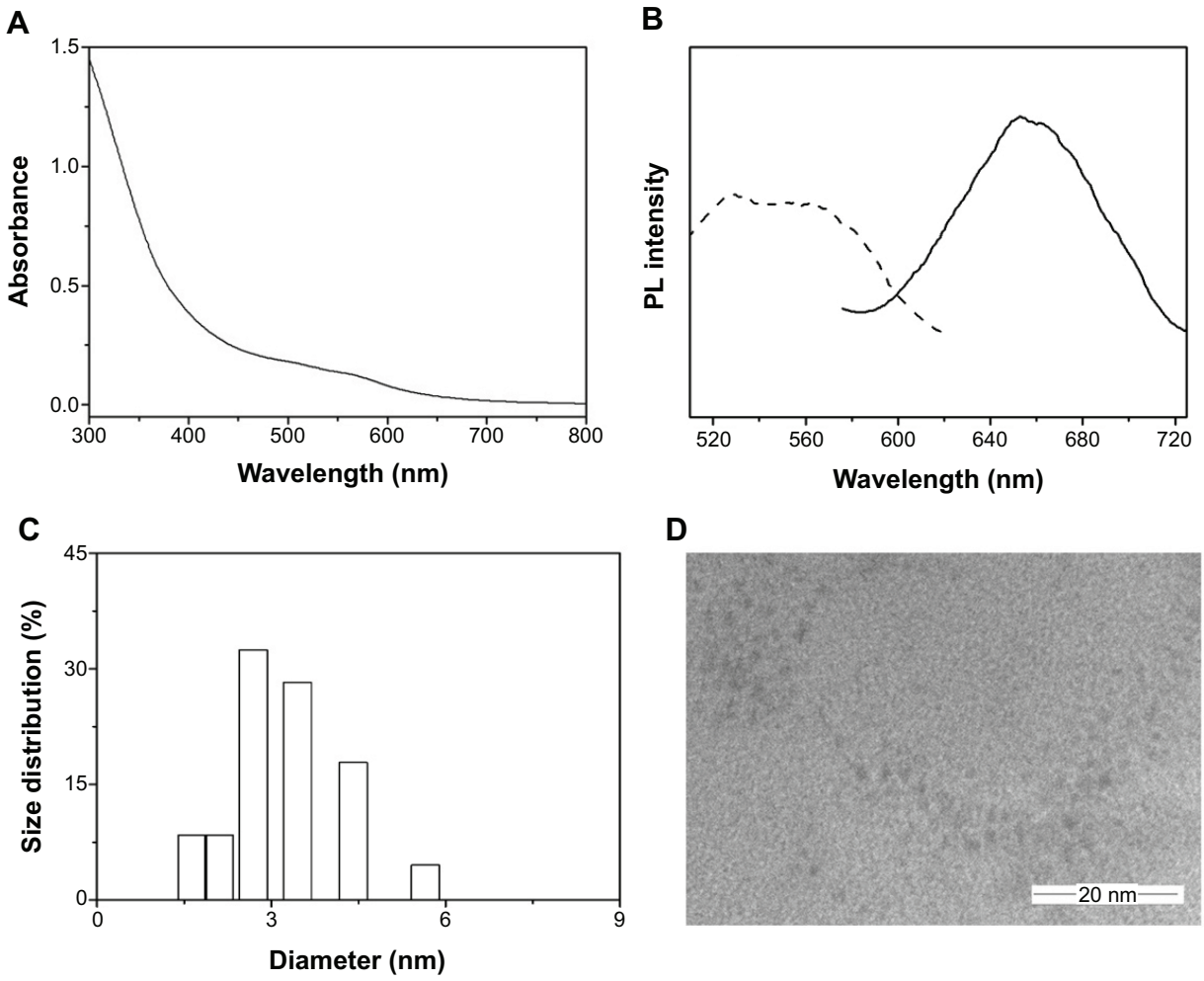

Figure 1 Characterization of dihydrolipoic acid–capped gold nanoclusters.
Notes: (**A**) UV–vis absorption spectrum, (**B**) photoluminescence spectrum (dashed line, emission at 660 nm; straight line, excitation at 550 nm), (**C**) size distribution, and (**D**) transmission electron microscopy images.
Abbreviations: PL, photoluminescence; UV-vis, ultraviolet visible.

(194.00%±7.78% versus control, $P<0.001$) at 72 hours. The fluorescence intensity then decreased markedly, and only 62.66%±3.45% ($P<0.05$) and 59.34%±2.82% ($P<0.05$) of the control were detected at the concentration of 100 μM and 125 μM, respectively.

Cell cycle in the presence of DHLA–capped Au NCs

We chose the low concentration (25 μM) and high concentration (100 μM) to determine the effects of DHLA–capped Au NCs on the cell cycle, and the results are shown in Figure 5. Compared to the control group, low concentration had almost no effect on the G1 (control: 54.69%, 25 μM: 54.09%), G2 (control: 5.18%, 25 μM: 4.77%), and S phase (control: 40.13%, 25 μM: 41.13%). The high concentration caused an apparent increase at the G1 phase (control: 54.69%, 100 μM: 58.18%), while the percentage of cells in the G2 phase was lower than that in the control (control: 5.18%, 100 μM: 4.18%), and the proportion in the S phase decreased (control: 40.13%, 100 μM: 37.63%).

Discussion

Due to the different quality between preparations of primary cells, cell lines (producing more reproducible results) are most often used for cytotoxicity screening.[17] We investigated the cytotoxicity of DHLA–capped Au NCs in the L02 and HepG2 cell lines at different exposure times. DHLA–capped Au NCs did not affect L02 cell viability even when exposed to 100 μM for 72 hours, but resulted in time- and concentration-dependent toxicity in the HepG2 cell line. The concentration of LDH in the culture medium of HepG2 cells increased after incubation for 72 hours, which was in accordance with the results of the cell viability assay. Intracellular ROS peaked at the concentration of 50 μM and then decreased with increasing concentrations of DHLA–capped

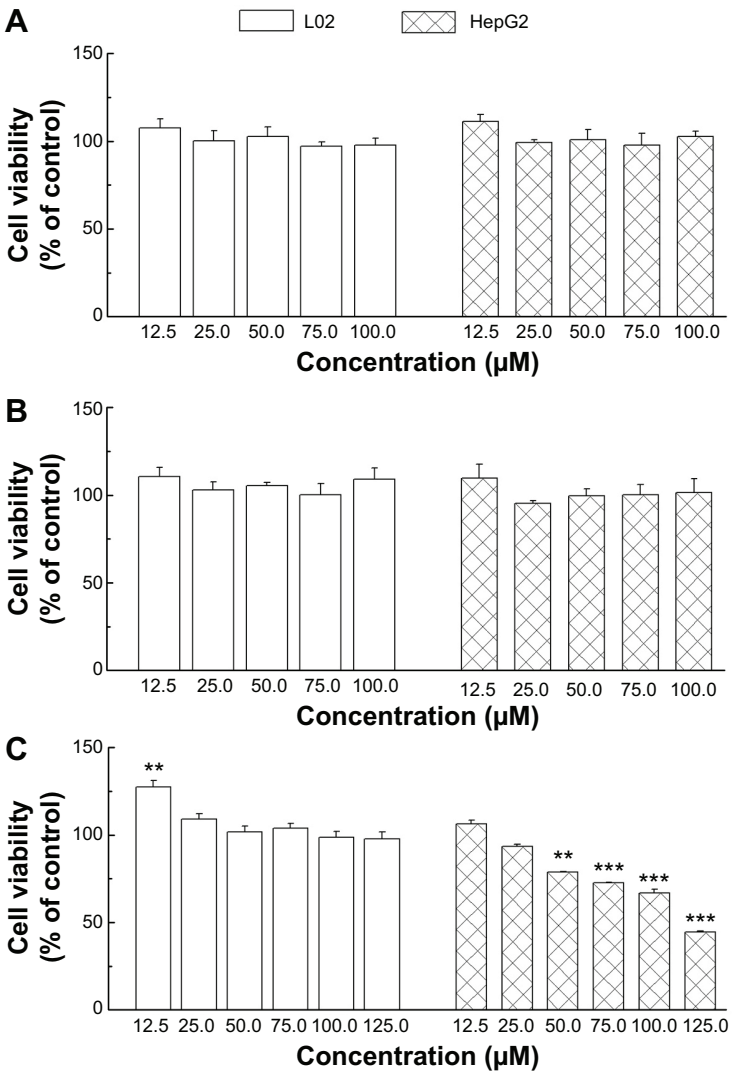

Figure 2 Cytotoxicity of dihydrolipoic acid–capped gold nanoclusters against L02 cells and HepG2 cells after (**A**) 24-h, (**B**) 48-h, and (**C**) 72-h exposure.
Notes: The viability was calculated relative to negative control. All data are presented as mean ± standard error of the mean (n=3). $^{**}P<0.01$ and $^{***}P<0.001$ verus control according to analysis of variance.
Abbreviation: h, hours.

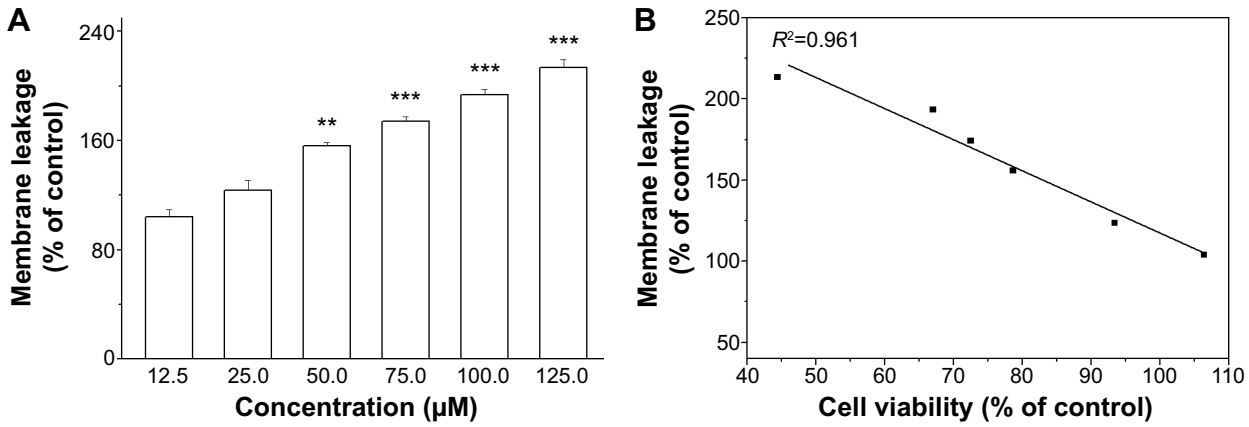

Figure 3 (**A**) LDH leakage and (**B**) correlation between cell viability and LDH levels in HepG2 cells after 72-h of incubation with different concentrations of dihydrolipoic acid–capped gold nanoclusters.
Notes: The LDH concentration was calculated relative to negative control. All data are presented as mean ± standard error of the mean (n=3). $^{**}P<0.01$ and $^{***}P<0.001$ verus control according to analysis of variance.
Abbreviations: h, hours; LDH, lactate dehydrogenase.

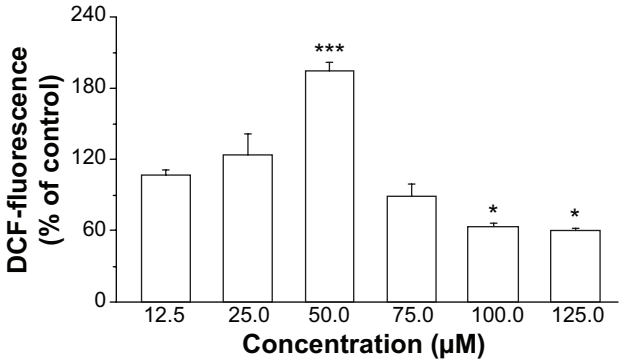

Figure 4 Formation of reactive oxygen species in HepG2 cells after 72-h incubation with different concentrations of dihydrolipoic acid–capped gold nanoclusters.
Notes: The dichlorofluorescein (DCF) fluorescence intensity was calculated relative to negative control. All data are presented as mean ± standard error of the mean (n=3). *$P<0.05$ and ***$P<0.001$ verus control according to analysis of variance.
Abbreviation: h, hours.

Au NCs. The proportion of HepG2 cells in the G1 phase increased following treatment with the high concentration of DHLA–capped Au NCs.

Due to their chemical stability and intrinsic photoluminescence, small Au NCs have shown great promise in cell labeling, biosensing, biomedical imaging, and drug delivery.[3,5] Gold is commonly known as an "innocent" element,[16] and numerous papers have reported that gold nanoparticles have low toxicity and good biocompatibility. Alkilany et al[18] reported that the apparent cytotoxicity of CTAB-capped gold nanorods in human colon carcinoma cells (HT-29) was caused by free CTAB in solution rather than the gold nanorods. Qiu et al[19] also concluded that CTAB molecules were the cause of Au nanorods cytotoxicity. However, Pan et al[20] found that 1.4-nm Au NCs had the lowest IC_{50} in a series of Au nanoparticles ranging in size from 0.8 nm to 15 nm, which was similar to previous reports which indicated that $Au_{55}(Ph_2PC_6H_4SO_3H)_{12}Cl_6$ caused serious cytotoxicity.[13] We found that DHLA–capped Au NCs affected liver cancer cells more than healthy cells, which is consistent with the cytotoxicity results obtained with Au_{55} reported by Tsoli et al.[13]

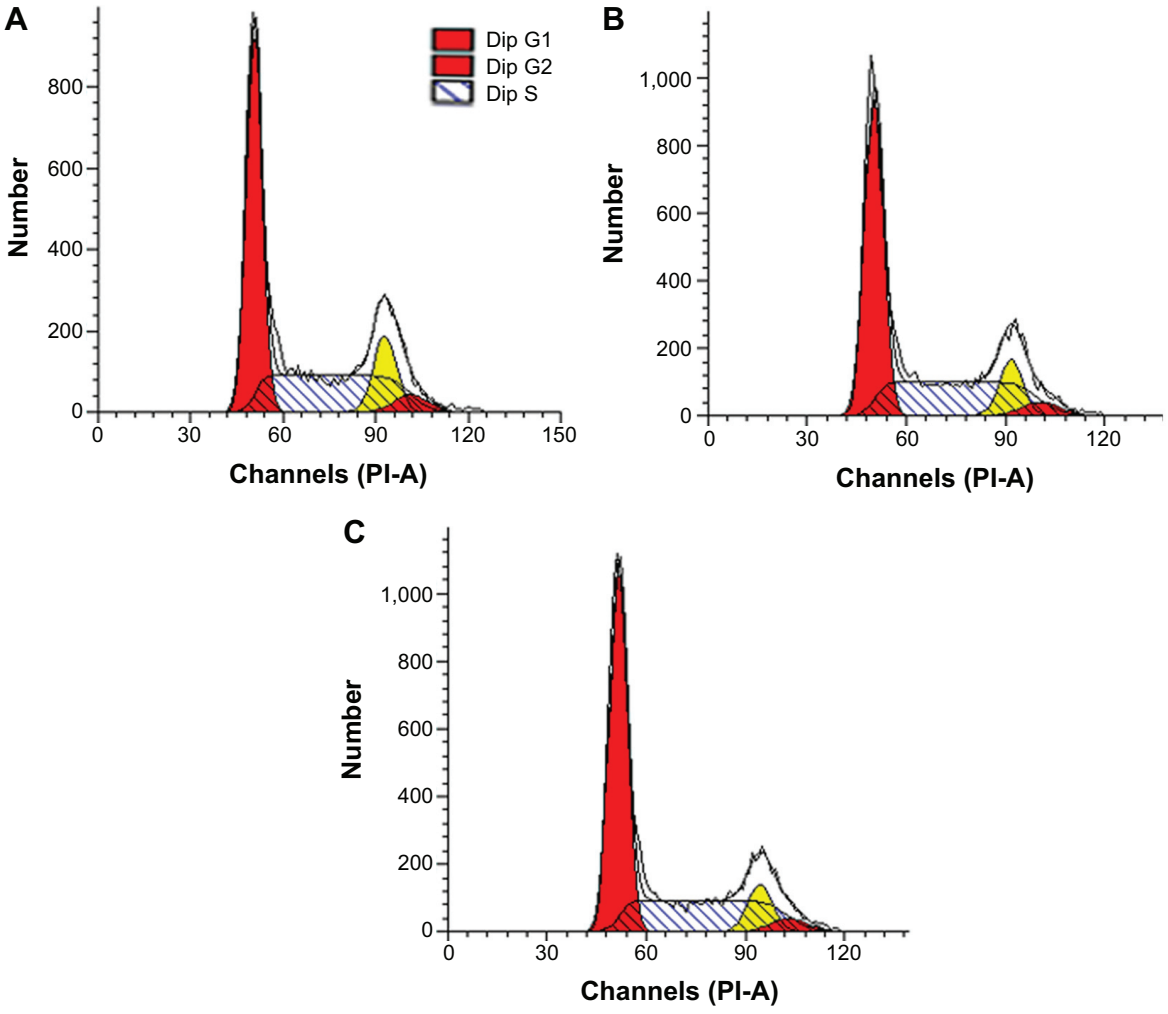

Figure 5 Cell cycle of HepG2 cells after 72-h incubation with (**A**) control and (**B**) 25 μM (**C**) and 100 μM dihydrolipoic acid–capped gold nanoclusters.
Abbreviation: h, hours.

This sensitivity of Au NCs indicated that they may induce anticancer effect when used in bioimaging and drug delivery. Li et al[21] reported that polypolex inhibited the growth of HepG2 cells and induced apoptosis, while keeping safe to L02 cell line at the same concentration. The authors deemed the different result of cytotoxicity was due to the different swollen ability between the tumor and normal cells.

Cell death or plasma membrane damage can cause cytoplasmic LDH leakage into the extracellular medium.[22] The concentration of LDH in the culture medium can reflect the integrity of the cell membrane.[22–24] The correlation between decreased cell viability and increased LDH activity after incubation with DHLA–capped Au NCs for 72 hours indicated that the reduction in cell number was related to membrane damage.

Oxidative stress following nanoparticle-induced ROS generation can cause external or internal cell damage, followed by decreased cell proliferation and may even lead to cell death via an apoptotic or necrosis pathway.[22,24,25] At relatively low concentrations, DHLA–capped Au NCs induced an increase in fluorescence in HepG2 cells after 72 hours of treatment, indicating the generation of ROS. Therefore, we suggest that decreased cell viability was related to oxidative stress. A previous report showed that the toxicity of many nanomaterials (eg, titanium dioxide, carbon nanotubes, zinc oxide) was induced by oxidative stress.[22] The decreased fluorescence of dichlorofluorescein at the concentration of 100 μM and 125 μM might be attributed to significant cell death.[26]

In the normal cell cycle, the DNA content changes regularly. Thus, we can determine the distribution of cell cycle phases through DNA staining and flow cytometry to calculate the percentages of cells in the G1, S, and G2 stages. G1 and G2 phases have two important checkpoints in the cell cycle, and a number of nanoparticles induce cell arrest in these phases.[27,28] The increased percentage of cells in the G1 phase suggested that DHLA–capped Au NCs induced HepG2 cell arrest in the G1 phase after high-dose treatment for 72 hours. This meant that cells had difficulty passing the checkpoint between the G1 phase and S phase,[19] which further reduced the cell viability.[27]

Conclusion

In conclusion, DHLA–capped Au NCs were synthesized using the one-pot synthesis method and cytotoxicity was assessed in the L02 normal human hepatic cell line and the HepG2 human hepatoma cell line. DHLA–capped Au NCs affected the HepG2 cell line more than the L02 cell line. The cytotoxicity of DHLA–capped Au NCs in the HepG2 cell line was related to LDH leakage and ROS generation, while cell viability decreased due to cell cycle arrest in the G1 phase after treatment for 72 hours.

Acknowledgment

This study was supported by the research funds from the National Science Foundation (grant number 21375052).

Disclosure

The authors report no conflicts of interest in this work.

References

1. Palmal S, Jana NR. Gold nanoclusters with enhanced tunable fluorescence as bioimaging probes. *Wiley Interdiscip Rev Nanomed Nanobiotechnol*. 2014;6(1):102–110.
2. Yang X, Gan L, Han L, Wang J, Wang E. Facile preparation of chiral penicillamine protected gold nanoclusters and their applications in cell imaging. *Chem Commun (Camb)*. 2013;49:2302–2304.
3. Shang L, Azadfar N, Stockmar F, et al. One-pot synthesis of near-infrared fluorescent gold clusters for cellular fluorescence lifetime imaging. *Small*. 2011;7(18):2614–2620.
4. Hu DH, Sheng ZH, Zhang PF, et al. Hybrid gold-gadolinium nanoclusters for tumor-targeted NIRF/CT/MRI triple-modal imaging in vivo. *Nanoscale*. 2013;5(4):1624–1628.
5. Sun C, Yang H, Yuan Y, et al. Controlling assembly of paired gold clusters within apoferritin nanoreactor for in vivo kidney targeting and biomedical imaging. *J Am Chem Soc*. 2011;133(22):8617–8624.
6. Chen Y, Zhou H, Wang Y, et al. Substrate hydrolysis triggered formation of fluorescent gold nanoclusters – a new platform for the sensing of enzyme activity. *Chem Commun*. 2013;49(84):9821–9823.
7. Qiao J, Mu X, Qi L, Deng J, Mao L. Folic acid-functionalized fluorescent gold nanoclusters with polymers as linkers for cancer cell imaging. *Chem Commun*. 2013;49(73):8030–8032.
8. Yue Q, Sun L, Shen T, Gu X, Zhang S, Liu J. Synthesis of fluorescent gold nanoclusters directed by bovine serum albumin and application for nitrite detection. *J Fluoresc*. 2013;23(6):1313–1318.
9. Tam JM, Tam JO, Murthy A, et al. Controlled assembly of biodegradable plasmonic nanoclusters for near-infrared imaging and therapeutic applications. *ACS Nano*. 2010;4(4):2178–2184.
10. Zhang X-D, Wu D, Shen X, Liu P-X, Fan F-Y, Fan S-J. In vivo renal clearance, biodistribution, toxicity of gold nanoclusters. *Biomaterials*. 2012;33(18):4628–4638.
11. Sharma V, Singh P, Pandey AK, Dhawan A. Induction of oxidative stress, DNA damage and apoptosis in mouse liver after sub-acute oral exposure to zinc oxide nanoparticles. *Mutat Res*. 2012;745(1):84–91.
12. Liu Y, Meyer-Zaika W, Franzka S, Schmid G, Tsoli M, Kuhn H. Gold-cluster degradation by the transition of B-DNA into A-DNA and the formation of nanowires. *Angew Chem Int Ed Engl*. 2003;42(25):2853–2857.
13. Tsoli M, Kuhn H, Brandau W, Esche H, Schmid G. Cellular uptake and toxicity of Au55 clusters. *Small*. 2005;1(8–9):841–844.
14. Oh E, Fatemi FK, Currie M, et al. PEGylated Luminescent gold nanoclusters: synthesis, characterization, bioconjugation, and application to one- and two-photon cellular imaging. *Part Part Syst Charact*. 2013;30(5):453–466.
15. Gómez-Lechón MJ, Castell JV, Donato MT. The use of hepatocytes to investigate drug toxicity. *Methods Mol Biol*. 2010;640:389–415.
16. Semmler-Behnke M, Kreyling WG, Lipka J, et al. Biodistribution of 1.4- and 18-nm gold particles in rats. *Small*. 2008;4(12):2108–2111.
17. Fröhlich E. Cellular targets and mechanisms in the cytotoxic action of non-biodegradable engineered nanoparticles. *Curr Drug Metab*. 2013;14(9):976–988.

18. Alkilany AM, Nagaria PK, Hexel CR, Shaw TJ, Murphy CJ, Wyatt MD. Cellular uptake and cytotoxicity of gold nanorods: molecular origin of cytotoxicity and surface effects. *Small*. 2009;5(6):701–708.
19. Qiu Y, Liu Y, Wang L, et al. Surface chemistry and aspect ratio mediated cellular uptake of Au nanorods. *Biomaterials*. 2010;31(30):7606–7619.
20. Pan Y, Neuss S, Leifert A, et al. Size-dependent cytotoxicity of gold nanoparticles. *Small*. 2007;3(11):1941–1949.
21. Li G, Ye L, Pan J, et al. Antitumoural hydroxyapatite nanoparticles-mediated hepatoma-targeted trans-arterial embolization gene therapy: in vitro and in vivo studies. *Liver Int*. 2012;32(6):998–1007.
22. Li L, Sun J, Li X, et al. Controllable synthesis of monodispersed silver nanoparticles as standards for quantitative assessment of their cytotoxicity. *Biomaterials*. 2012;33(6):1714–1721.
23. Holder AL, Goth-Goldstein R, Lucas D, Koshland CP. Particle-induced artifacts in the MTT and LDH viability assays. *Chem Res Toxicol*. 2012;25(9):1885–1892.
24. Lin W, Huang Y-W, Zhou X-D, Ma Y. Toxicity of cerium oxide nanoparticles in human lung cancer cells. *Int J Toxicol*. 2006;25(6):451–457.
25. Jeong YS, Oh W-K, Kim S, Jang J. Cellular uptake, cytotoxicity, and ROS generation with silica/conducting polymer core/shell nanospheres. *Biomaterials*. 2011;32(29):7217–7225.
26. Saquib Q, Al-Khedhairy AA, Ahmad J, et al. Zinc ferrite nanoparticles activate IL-1b, NFKB1, CCL21 and NOS2 signaling to induce mitochondrial dependent intrinsic apoptotic pathway in WISH cells. *Toxicol Appl Pharmacol*. 2013;273(2):289–297.
27. Song D, Zheng L, Shen S, Chen X. Cytotoxicity of ammonium hexafluorosilicate on human gingival fibroblasts. *Toxicol In Vitro*. 2013;27(8):2149–2155.
28. Wei L, Tang J, Zhang Z, Chen Y, Zhou G, Xi T. Investigation of the cytotoxicity mechanism of silver nanoparticles in vitro. *Biomed Mater*. 2010;5(4):044103.